Constructing a Seasonal and Sub-seasonal Variance Budget for OCO-2 XCO_2 for North America and Adjacent Ocean Basins

We construct a seasonal and sub-seasonal variance budget for OCO-2 XCO_2 over North America that reflects a combination of carbon fluxes, atmospheric transport, and potential instrument or algorithm biases.

1. Kayla Mitchell, UVA 2. Scott Doney, UVA 3. Gretchen Keppel-Aleks, MICH

Image: NASA/JPL

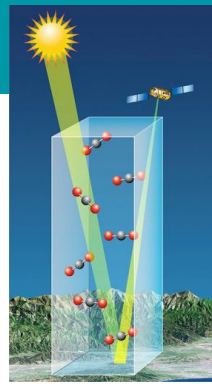

This variance budget of XCO_2 from NASA's Orbiting Carbon Observatory-2 (OCO-2) includes:

- Amplitude and timing of the XCO_2 seasonal cycle
- Synoptic-scale XCO_2 variance
- Mesoscale & finer XCO_2 variance
- Explained & unexplained high frequency XCO_2 variance
- Spatial correlation range of high frequency XCO_2 variance
- Skewness & kurtosis of sub-seasonal XCO_2
- Variance by operation mode and surface type

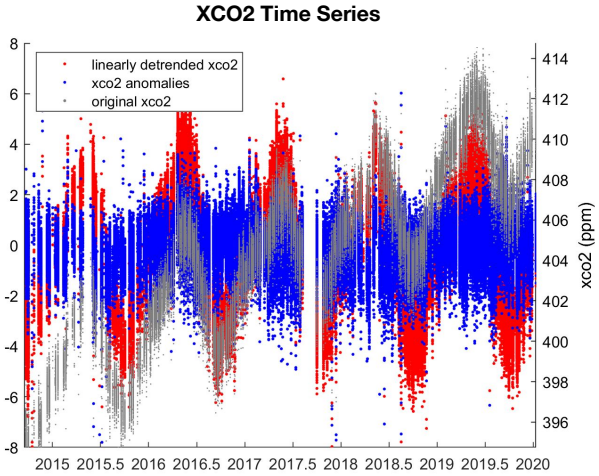

1. XCO_2 data are analyzed in 5x5 degree bins. For one bin over Hawaii, this plot shows the original XCO_2, long-term linearly detrended XCO_2, & sub-seasonal XCO_2 anomalies.

XCO_2: total atmosphere column averaged CO_2 dry air mole fraction (ppm)

We observe significant large-scale patterns, regional features, and land-ocean contrasts in OCO-2 XCO_2 variance. In further research efforts, we will attribute these patterns to real geophysical drivers (such as surface fluxes and atmospheric transport) or error induced by retrieval covariates such as topography, albedo, and aerosols.

Methods

The full OCO-2 V9 XCO_2 time series (2014-2019) is quality-filtered and long-term temporally detrended.

2. XCO_2 are grouped into 5x5 degree bins. For each bin, the mean XCO_2 concentration is removed and the seasonal cycle is fit and detrended.
3. A 6 month low pass filter is used to remove interannual variations from the sub-seasonal XCO_2 anomalies.

4-5. For each individual orbit pass through each bin, sub-seasonal anomalies are 250 km high pass filtered to separate synoptic from mesoscale & finer variance.

6. Semivariograms are computed on the final high pass anomalies and fitted to estimate the sill (ppm^2) **(A)**, nugget (ppm^2) **(B)**, and correlation range (km) **(C)** of along-track high frequency XCO_2 variance. Semivariograms measure spatial dependence between observations as a function of distance. Along-track spatial correlation in XCO_2 is driven by natural processes that vary gradually with distance (like weather systems).

2.

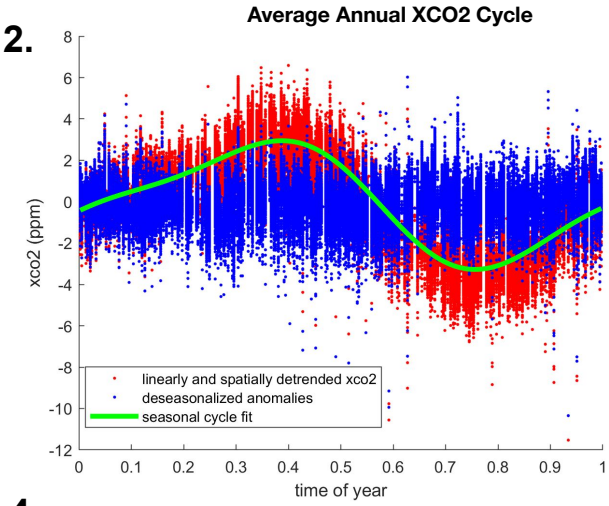

3.

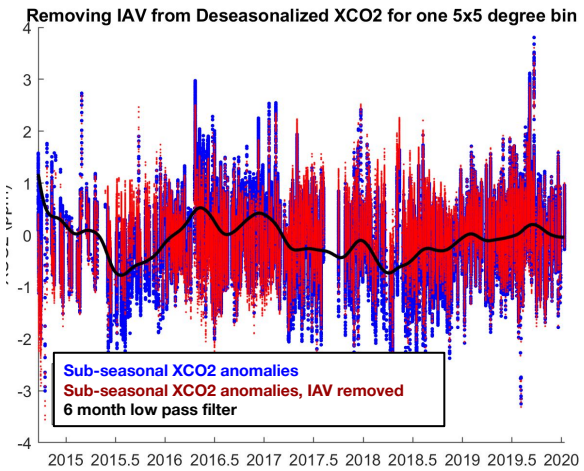

4.

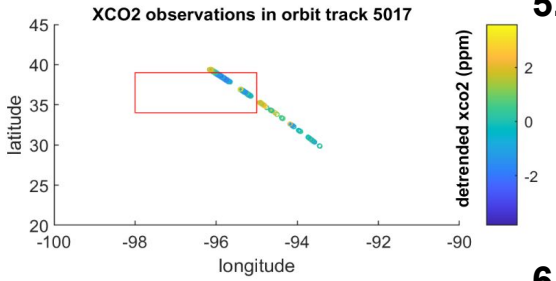

5.

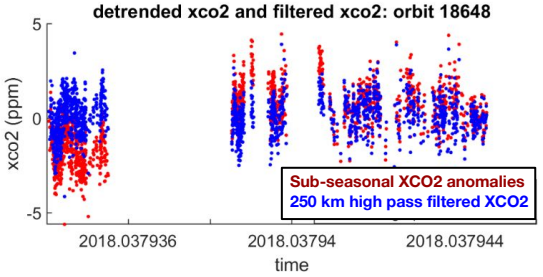

6.

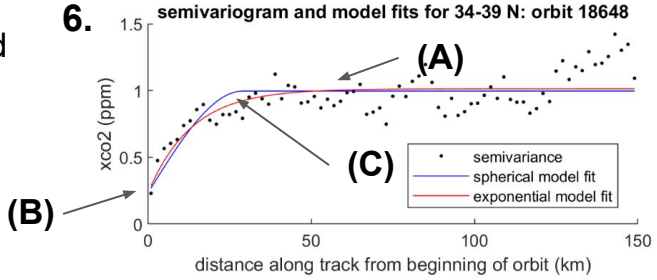

XCO_2 Means and Seasonal Cycle

7. The increasing north-south gradient in mean detrended XCO_2 is shaped by growing season carbon drawdown in the northern latitudes.

8. Seasonal amplitudes are greater in the north & follow mean wind patterns across the northern continent. We observe patterns in XCO_2 amplitudes are inconsistent with surface flux seasonality, showing that seasonal XCO_2 variance reflects large-scale circulation as well as regional fluxes.

9-10. The seasonal cycle maximum occurs during April-May and minimum occurs August-September for most bins. Northern bins with greater amplitudes tend to peak earlier in the year. XCO_2 lags behind the surface CO_2 seasonal cycle.

7.

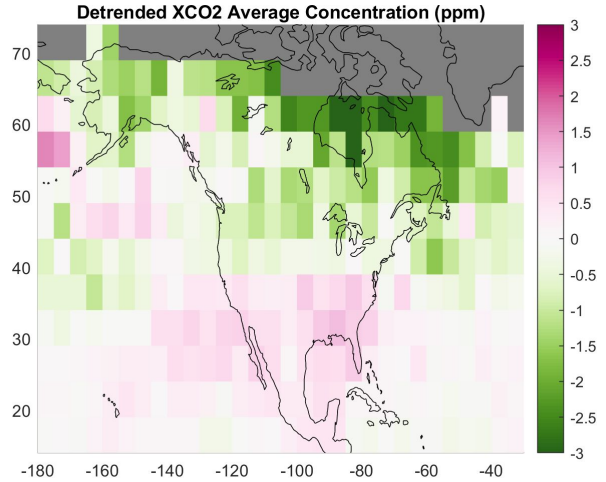

8.

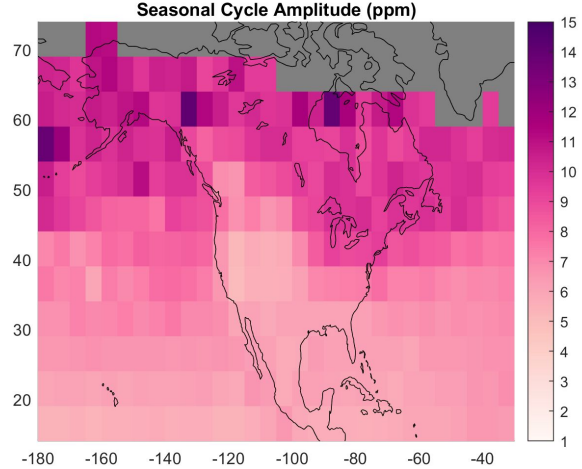

9.

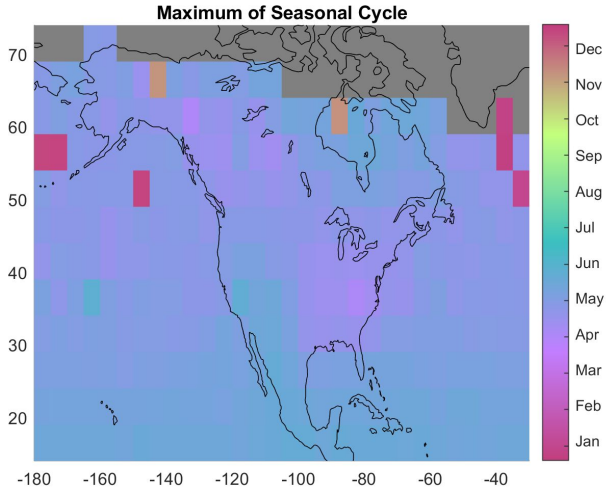

10.

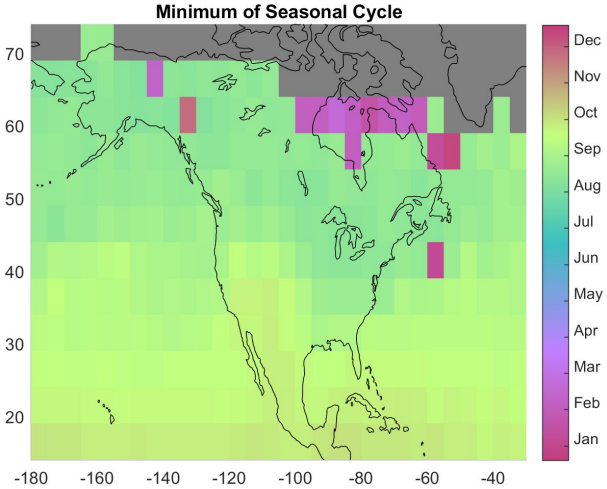

Sub-seasonal variance divided into synoptic-scale & mesoscale (<250 km) variance

Note: Maps are presented on a log scale to better observe relative variance patterns across the domain.

11. Synoptic-scale variance dominates the sub-seasonal variance budget, ranging from ~0.5-4 ppm^2. Large-scale/zonal patterns are more pronounced.

12. Mesoscale variance ranges from ~0.3-2 ppm^2. Regional patterns are more pronounced.

Both scales of variance are greater over land than ocean.

Aggregated sub-seasonal XCO_2 skewness & kurtosis

13-14. Skewness is dominantly negative over the ocean and slightly positive over land. All bins are have greater kurtosis than a normal distribution (K=3).

11.

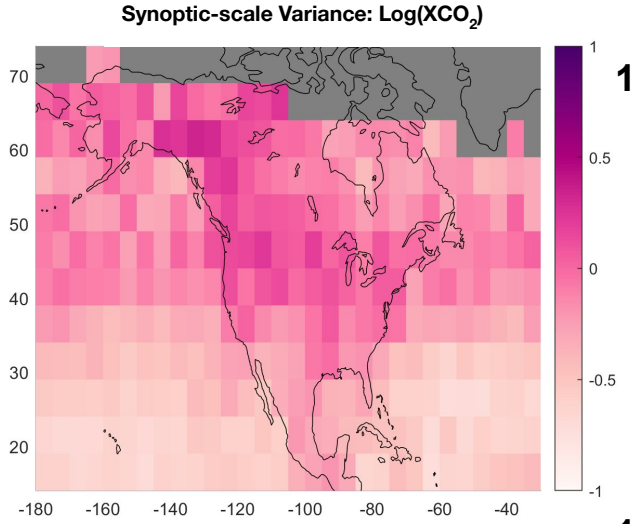

12.

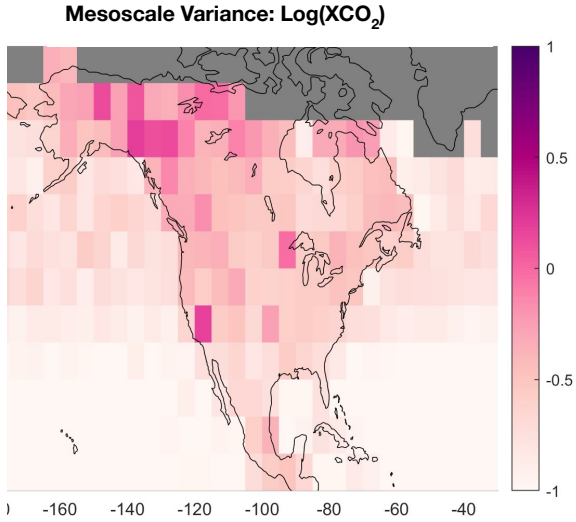

13.

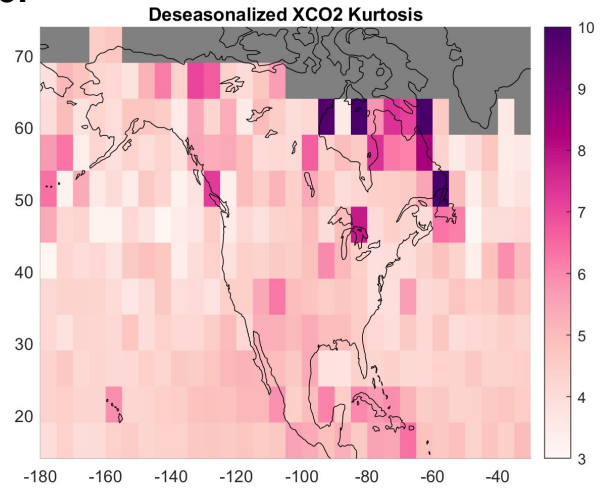

14.

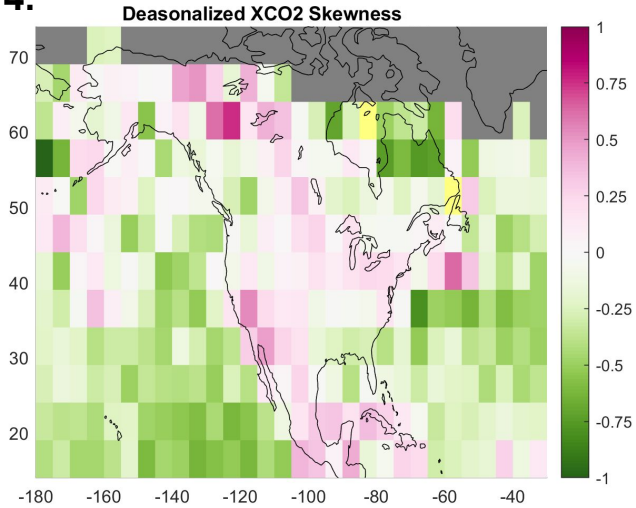

Semivariogram analysis of high frequency (mesoscale & finer) along-track XCO_2 variance

15. Semivariance of high pass filtered XCO_2 along one orbit through one bin. 16-18 show weighted averages of all sill, nugget, and range estimates.
16. Sill: total spatially coherent mesoscale and finer XCO_2 variance.
17. Nugget: underlying variance of the data (random error/noise).
18. Range: distance at which two observations are unrelated. XCO_2 ranges are ~10 km greater over the ocean.

Short ranges over land are too small for the high frequency variance to be totally driven by mesoscale weather systems. This suggests that retrieval covariates (aerosols, albedo, roughness) could contribute to high frequency variance in these regions.

15. ★sill (~1 ppm^2) ☆nugget (~0.3 ppm^2) ★range (~30 km)

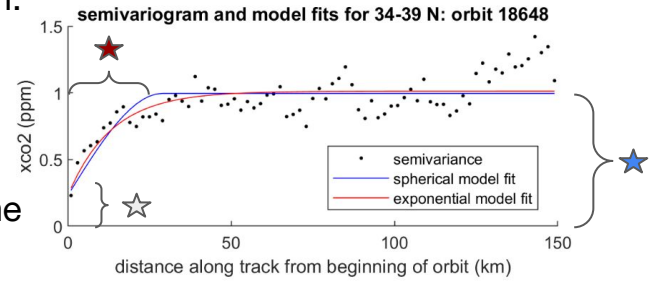

16.

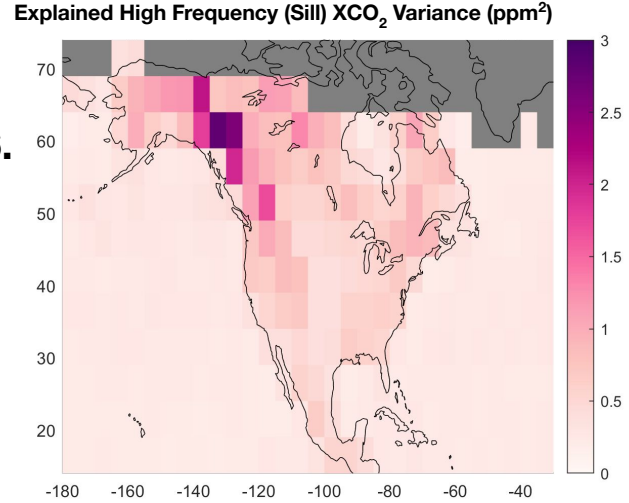

17.

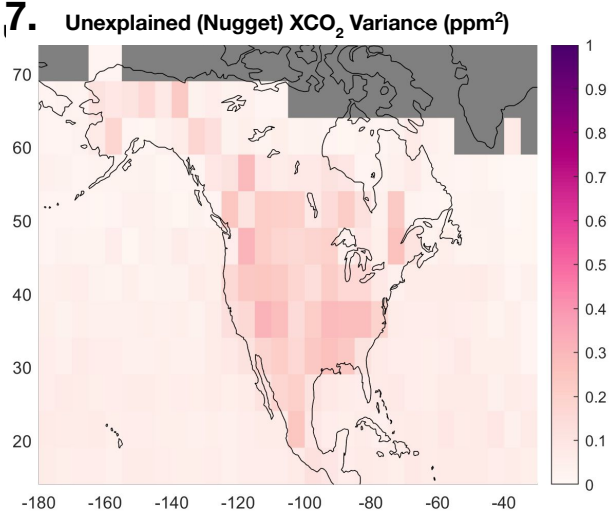

18.

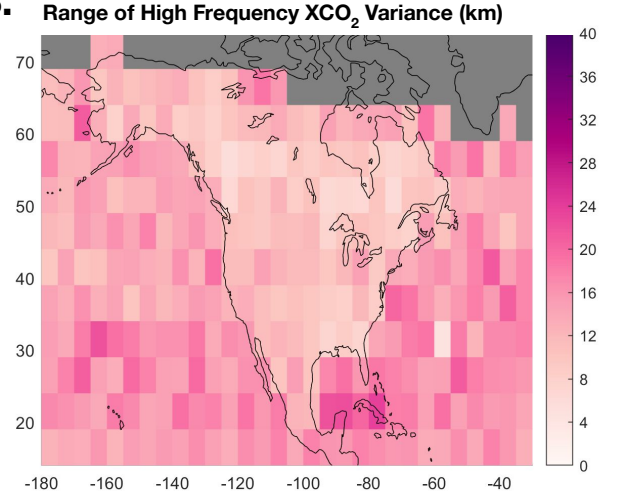

Variance on all sub-seasonal scales is greater over land.

We are trying to understand to what extent retrieval issues contribute to this pattern. Ocean fluxes are generally less variable, but the land-ocean contrast we observe seems too prominent to be explained by fluxes or transport alone.

What is causing greater sub-seasonal variance over the northwestern continent?

19. Surface roughness (left), which can induce erroneous variance in retrievals, exhibits a strong spatial correlation with sub-seasonal variance. We are analyzing V10 data to evaluate if bias correction reduced this variance. It is also possible that roughness is actually driving more atmospheric mixing of XCO_2 concentration gradients.

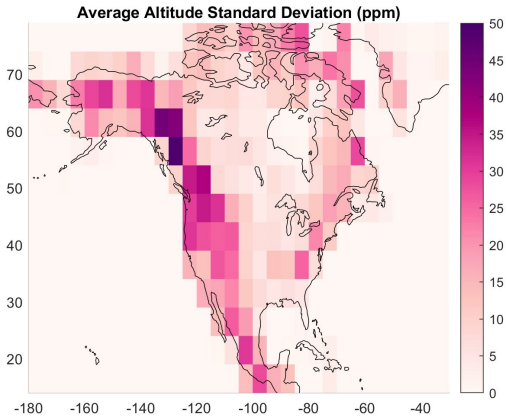

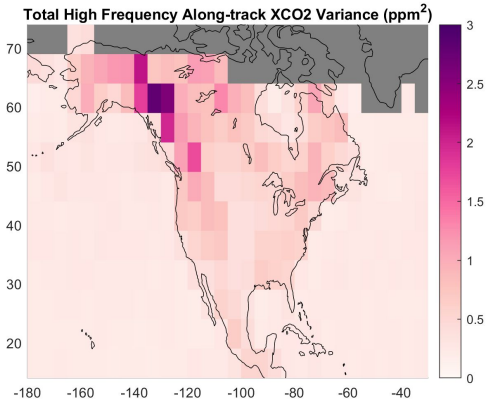

Operation Mode	variance (ppm^2)	skewness	kurtosis
nadir	1.91	0.14	5.77
land glint	1.87	0.08	5.31
ocean glint	0.78	-0.05	4.61
Surface Type			
land	1.91	0.18	5.40
water	0.78	-0.05	4.61
mixed	2.70	-0.02	6.77

Sub-seasonal XCO_2 anomaly variance by satellite operation mode and retrieval surface type

Nadir (only retrieves over land) and land glint modes have greater XCO_2 variance and kurtosis than ocean glint mode. Mixed surface type retrievals have the greatest sub-seasonal variance and kurtosis on average, followed by land retrievals. Sub-seasonal variance for one bin over Lake Michigan: Land: 2.03 ppm^2 Water: 1.23 ppm^2 Mixed: 2.61 ppm^2